ACS APPLIED POLYMER MATERIALS

pubs.acs.org/acsapm
Article

3D Printing of Vinylogous Urethane-Based Methacrylic Covalent Adaptable Networks by Vat Photopolymerization

Laura Ballester-Bayarri, Alodi Pascal, Jon Ayestaran, Alba Gonzalez, Nicholas Ballard,* and Robert Aguirresarobe*

Cite This: ACS Appl. Polym. Mater. 2024, 6, 2594−2603
Read Online

ACCESS | Metrics & More | Article Recommendations | Supporting Information

ABSTRACT: Covalent adaptable networks (CANs) have the potential to combine the excellent mechanical properties of traditional thermoset materials with the reprocessability of traditional thermoplastics. However, the processing of CANs using common techniques for thermoplastics has proven challenging. In this work, the 3D printing of reprocessable CANs with controlled shape is reported using vat photopolymerization (VP). Using a vinylogous urethane-containing methacrylic cross-linker, a series of resins containing nonreactive and reactive diluents are described. The resin viscosity can be easily tuned by the relative amount of diluent to functional cross-linker such that the viscosity of commercial resins can be easily achieved. By studying the curing kinetics using Jacob's equation, optimal printing conditions are found that allow for high-resolution printing with limited shrinkage. In addition, due to the presence of dynamic bonds in the final material, it is shown that the final printed piece can be reprocessed at high temperatures and can even be recycled into a second-generation resin that can be reprinted.

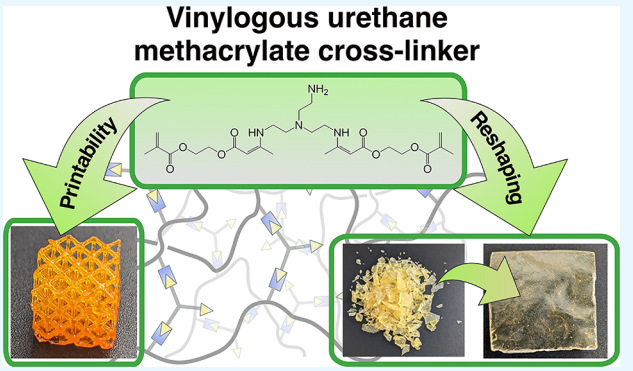

KEYWORDS: *vinylogous urethane, vat photopolymerization, additive manufacturing, reprocessability, associative CANs*

INTRODUCTION

Covalent adaptable networks (CANs) are cross-linked polymer networks that ideally combine the processability of thermoplastics with the mechanical properties of thermosets.[1−5] In these systems, dynamic covalent bonds are incorporated into the network structure such that, upon the application of external stimuli, the network can adapt to applied stress through changes in the network topology.[6] This change permits the material to rearrange and, eventually, to flow, making both reprocessing and recycling of CANs possible.[2] A number of dynamic covalent systems have been reported for use in CANs that differ both in the nature of the chemistry involved and in the mechanism of bond exchange, which can be either dissociative or associative.[7−11]

Manufacturing represents one of the greatest challenges in CANs and efforts have focused on applying conventional processing techniques to these types of materials. For example, Erice et al.[12] developed a polythiourethane thermoset and showed that it can be processed by injection molding at 180 °C where the dissociative exchange of the thiourethane group can occur. Similarly, Du Prez and co-workers reported the extrusion of vinylogous urethane-based associative networks by accelerating bond exchange through catalysis.[13] An alternative route around this problem is to produce the vitrimer in situ during processing, such as the reactive extrusion approach of Qiu et al.[14] and Li et al.[15] for poly(ethylene terephthalate) and cellulose-based vitrimer, respectively, or the reactive blending system reported by Montarnal and co-workers.[16]

Due to the challenges associated with the processing of CANs, the shape complexity of the final processed materials is generally limited, and therefore, new fabrication techniques to process CANs must be sought. In this sense, much of the effort has been focused on additive manufacturing (AM) technologies.[17] To date, the printing of dynamic networks has been applied to shape memory,[18−20] stimuli-responsive,[6] self-healing[21] and soft robotic applications.[22] One of the most established AM technologies are material extrusion 3D printing. The manufacturing concept relies on the selective deposition of fluidized material extruded through a printing nozzle into a printing platform. Several examples of material extrusion AM of CANs can be found in the literature.[23] As representative examples, Saito and co-workers produced closed-loop AM using imine exchange in acrylonitrile

Received: November 14, 2023
Revised: February 14, 2024
Accepted: February 14, 2024
Published: February 26, 2024

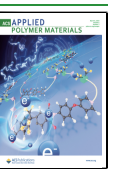

https://doi.org/10.1021/acsapm.3c02777
ACS Appl. Polym. Mater. 2024, 6, 2594−2603

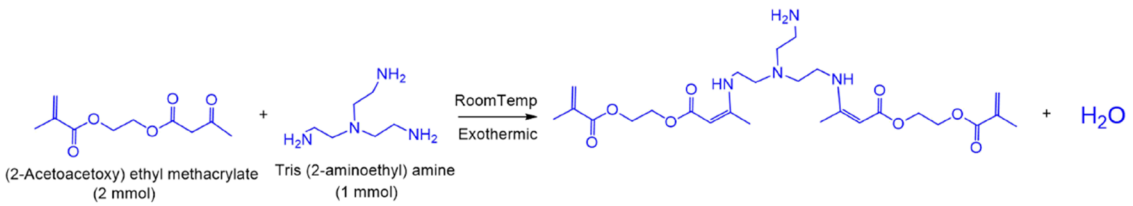

Figure 1. Methacrylated vinylogous urethane cross-linker formation was through an exothermic reaction at room temperature.

Table 1. Recipes of for the Resin Formulations Used in This Work

	AAEMA		TREN		DILUENT			DMPA
code	(g)	(mmol)	(g)	(mmol)	(g)	(mmol)	diluent (wt %)	(mg)
DMSO42	7.74	36.13	2.50	17.096	7.35	94.07	42	5
DMSO20	7.70	35.94	2.54	17.37	3.53	45.18	20	
GLYCOL23	9.97	46.54	3.49	23.86	4.35	26.81	23	5
GLYCOL29	10.11	47.19	3.47	23.73	5.48	33.78	29	
GLYCOL33	9.96	46.49	3.40	23.25	6.29	38.77	33	
BMA27	1.00	4.67	0.35	2.40	0.5	3.52	27	5
BMA45	1.00	4.67	0.35	2.40	1.10	7.75	45	
BMA50	1.00	4.67	0.35	2.40	1.30	9.14	50	
BMA60	1.00	4.67	0.35	2.40	2.00	14.06	60	
2EHMA50	1.00	4.67	0.35	2.40	1.30	67.35	50	

butadiene styrene CANs.[24] Advincula and co-workers produced 3D parts by using vinylogous urethane-modified polyureas. Similarly, Terentjev and co-workers developed 3D printable filaments based on polypropylene-containing thiol-anhydride exchangeable cross-links[25] and, more recently, expanded the concept using dynamic transesterification reactions.[26]

One alternative to material extrusion 3D printing is vat photopolymerization (VP).[18,27,28] In this technology, a cross-linked 3D shape is produced in situ by photopolymerizing a polymer resin. In this case, the printing process involves the application of low shear in comparison with material extrusion AM (around 5−20 s^{-1} during submerging/withdrawing) and allows for the in situ polymerization of polymer network, offering a route to 3D printing of CANs.[17,29,30] It is important to note that the printing of dynamic covalent networks still presents a challenge, as the material must fulfill several requirements to ensure printability.[31] First, the viscosity of the initial resin must be sufficiently low to allow for efficient recoating during the printing process.[32] Second, the cross-linking process should be light-activated, and the dynamic bond should not interfere in this process. Finally, the reaction kinetics of the cross-linking process has to be fast enough in order to provide a good spatial resolution.[29] Based on these prerequisites, most VP systems rely on radical photopolymerization processes, although examples of other initiation systems, such us thiol−ene or cationic initiations can be found in the literature.[32,33] These reactions differ from step-growth polymerization of most of the dynamic network examples. In order to achieve both printability and dynamic characteristics, one alternative can be to incorporate dynamic bonds into acrylic cross-linkers. Thus, Sample and co-workers[34] designed a dyallyl boronate cross-linker for its use using thiol-ene chemistry. Dunn and co-workers[35] produced dynamic networks based on transesterification, using acrylate terminated epoxy resin and a radical photpolymerization. Zhang and co-workers developed a polythiourethane cross-linker and used the resulting 3D CAN in self-heling and shape memory applications.[36] Similarly, 3D-printed sacrificial scaffolds and recyclable resins have been developed using acetal[37,38] and hindered urea[39−41]-based CANs.

In this work, we report the development of a VP system for the 3D printing of methacrylate-based vitrimers using a methacrylated vinylogous urethane cross-linker. First, the potential capabilities of the methacrylated vinylogous urethane cross-linker for 3D printing are discussed. Subsequently, the cross-linking process and VP of the vinylogous urethane cross-linker when mixed with a monofunctional methacrylic monomer (*n*-butyl methacrylate) are explored, targeting spatial control of the printing process. Finally, the potential ability to utilize the dynamic nature of the vinylogous urethane group to permit the reprocessing of the printed material is discussed.

EXPERIMENTAL SECTION

Materials. *n*-Butyl methacrylate (n-BMA, 99%), (2-acetoacetoxy) ethyl methacrylate (AAEMA, 95%), tris(2-aminoethyl) amine (TREN) (96%), di(propylene glycol) dimethyl ether (Proglyde DMM), 2-ethylhexyl methacylate (2-EHMA), and hexylamine were provided by Sigma-Aldrich. Ethylenediamine (99%) was provided by ThermoScientific. Dimethyl sulfoxide (DMSO) was provided by Fluka. 1, 4-dioxane was provided by Panreac. Sudan I was provided by Tokyo Chemical Industry. 2,2-Dimethoxy-2-phenylacetophenone (DMPA) was used as the initiator. All of the reagents were used as received.

Synthesis. The synthesis of the methacrylated vinylogous urethane cross-linker was carried out in one step (see Figure 1) based on the synthesis developed by Ballester-Bayarri et al.[42] The cross-linker was synthesized by the addition of tris (2-aminoethyl) amine (TREN) to (2-acetoacetoxy) ethyl methacrylate (AAEMA) in a round-bottomed flask at room temperature. The as-synthesized monomer was dissolved in a series of reactive and nonreactive diluents in order to generate a range of resins (Table 1). In all cases, an excess of amine was added in a 2:1 mol ratio (AAEMA:TREN) to allow the presence of free amine groups to give a polymer the further dynamic behavior.[42,43]

Characterization. The vinylogous urethane cross-linker was characterized by ^{13}C nuclear magnetic resonance (^{13}C NMR) with a Bruker Advance 400 spectrometer. The NMR chemical shifts were

https://doi.org/10.1021/acsapm.3c02777
ACS Appl. Polym. Mater. 2024, 6, 2594−2603

reported as δ in parts per million (ppm) relative to the traces of nondeuterated solvent ($CDCl_3$).

Rheological experiments were performed in an ARES-G2 rheometer from TA Instruments. Frequency sweeps were performed in shear geometry with 8 mm diameter plates under linear viscoelastic conditions in which the storage modulus and the loss modulus of the samples were determined. Stress relaxation measurements were performed to obtain the relaxation modulus (G(t)) in shear, using plates with 8 mm of diameter under linear viscoelastic conditions. The samples had a thickness between 0.6 and 1 mm. At least three repetitions were made to check the reproducibility of the experiment. Photorheology experiments were performed using an AR-G2 rheometer from TA Instruments under linear viscoelastic conditions with a light emission accessory at 365 nm of variable intensity. Twenty millimeter diameter plates were used with an acrylic bottom plate to allow the irradiation to pass through. Gap values were around 200 and 350 μm, and the measurements were carried out at room temperature varying the irradiation intensity to study the curing kinetics.

Viscosity measurements were carried out with an Anton Paar MCR101 rheometer at different shear rates using concentric cylinders of 10 and 17 mm of diameter. The tests were carried out at 25 °C, and the shear rates used were from 1 to 1000 s^{-1}.

Differential scanning calorimetry (DSC) A Q2000 DSC from TA Instruments with an Omnicure 52000-XLA irradiation system was used to study the photocuring of the resins. The wavelengths were around 320 and 500 nm. The UV light intensity was 116 mW/cm^2, and nitrogen was employed as purge gas. Photocalorimetry studies were conducted in order to estimate the conversion of the curing reaction and the polymerization rate. The kinetics were determined following the method reported by Harikrishna.[44]

Samples were reprocessed in Collin P200E compression molding machine under the following conditions: (1) preheating the mold for 2 min at 140 °C; (2) heating the sample at 140 °C until a pressure of 200 bar increasing 50 bar each 15 s; (3) heating the sample at 140 °C during 2 min at 200 bar of pressure; and finally (4) cooling the sample during 5 min.

Scanning electronic microscopy (SEM) was performed using a TM3030 Plus (Hitachi) with an acceleration voltage of 15 kV. Prior to imaging, the samples were coated in a Sputter Coater Microscience Division SC500 for 30 s at 15−20 mA.

Gel content was measured by Soxhlet extraction with tetrahydrofuran under reflux for 24 h. Following this step, samples were dried in an oven for 1 day at 65 °C. The gel content values were calculated using the following expression:

$$\text{Gelcontent}(\%) = \frac{W_4 - W_1}{W_2 - W_1} \times 100$$

where W_4 is the mass of the polymer after being dried in the oven overnight, W_1 is the filter mass, and W_2 is the mass of the polymer before the Soxhlet process.

Cure depth measurements were carried out using the following procedure: a droplet of the desired resin was placed on top of a 0.17-mm thick microscope slide, and a 2-mm circular spot was projected with varying intensity and exposure times (25−100 s) in the printer. After projection, uncured ink was rinsed, and the layer was carefully dried with acetone to remove the excess of resin. The cured film thickness (C_d) was measured using a micrometer. The corresponding measured C_d values for each E are represented, resulting in the so-called Jacobs working curves.

AM was carried out in an ASIGA MAX UV printer. The printer irradiates UV light centered at 385 nm and has a resolution of 65 μm in the XY axis and 1 μm in the Z axis. In order to modify the models taken from the Thingiverse Web site, the Asiga Composer software was used. With this software, the dimensions of the pieces, the irradiation time, and the intensity were determined. In Table 2, the printing conditions are shown for the chosen compositions. The printed models were designed using Autodesk Inventor © and Blender softwares.

Table 2. Optimum 3D Printing Conditions

	exposure time (s)	layer thickness (mm)	temperature (°C)	irradiance (mW/cm^2)
DMSO42	60	0.05	25	20
GLYCOL29	77			
BMA45	25			
BMA50	30			
2EHMA50	2			

Spectral output of the light sources of photorheology and VP was measured by using a StellarNet Black-Comet spectrometer with a wavelength acquisition range of 190−850 nm. Spectra of the different light sources are shown in Figure S1.

Mechanical characterization was carried out by measuring the stress−strain curves in an Instron 5569 universal test machine using ASTM D638- Type V specimens and a crosshead speed of 10 mm/min. A minimum of five specimens were tested for determining the mechanical properties.

Aminolysis was carried out in order to check the dynamic behavior of the resin. In one vial, a printed sample of BMA45 (0.14 g) was added to 7 g of 1,4-dioxane for 1 day at 60 °C. In another vial, a printed sample of BMA45 (0.14 g) was added to 1.4 g of hexylamine and 7 g of 1,4-dioxane for 1 day at the same temperature. A recyclability experiment was carried out using the printed piece of BMA45 but instead of adding a monofunctional amine, a bifunctional amine was used; a 1.1 g 3D printed cube of BMA45 was immersed in 5.5 g of ethylenediamine at room temperature during 5 days. Once the printed sample was dissolved, 0.35 g of the resulting solution was taken and mixed with 2.5 g of AAEMA and 2.5 g n-BMA to obtain another resin with appropriate viscosity. The AAEMA content was calculated in a 2:1 mol ratio respect to added ethylenediamine.

RESULTS AND DISCUSSION

As shown in previous work, the mixture of AAEMA and TREN leads to the formation of a methacrylated vinylogous urethane-containing cross-linker (see Figures 1 and S2).[42] In a first step, the printing capabilities of the synthesized vinylogous urethane cross-linker were studied. Due to its highly viscous nature, a solvent (dimethyl sulfoxide, DMSO) and a plasticizer Proglyde DMM (named here as GLYCOL) were added in different amounts in order to produce a photo resin with viscosity suitable for printing. As can be seen in Figure S3, DMSO20 and GLYCOL23 showed high viscosity values and pseudoplastic behavior, while DMSO42 and GLYCOL29 and 33 showed Newtonian behavior with values within the conventional processing window for vat photopolimerization.[30] The capacity of the samples to photo-cross-link was determined by photorheology measurements, as shown in Figure 2a. Both DMSO and GLYCOL-based samples produced a very fast gelation of the material when the sample was irradiated, having similar gel points even though the irradiation intensity varied. However, it is to note that the modulus of GLYCOL29 is significantly lower than the one of DMSO42 due to the plasticizing effect of Proglyde DMM.

The key feature of the developed cross-linker is the presence of dynamic bonds, which should allow for a vitrimer-like behavior of the cured material. To explore this point, stress relaxation measurement were conducted at temperatures ranging from 160 to 190 °C. As shown in Figure 2b, stress relaxation occurred in the materials, and the relaxation times decreased at higher temperatures. Here again, the plasticizing effect of the GLYCOL is evident as the initial relaxation modulus is 2 orders of magnitude below that of the DMSO-based sample and relaxation occurred at lower temperatures.

https://doi.org/10.1021/acsapm.3c02777
ACS Appl. Polym. Mater. 2024, 6, 2594−2603

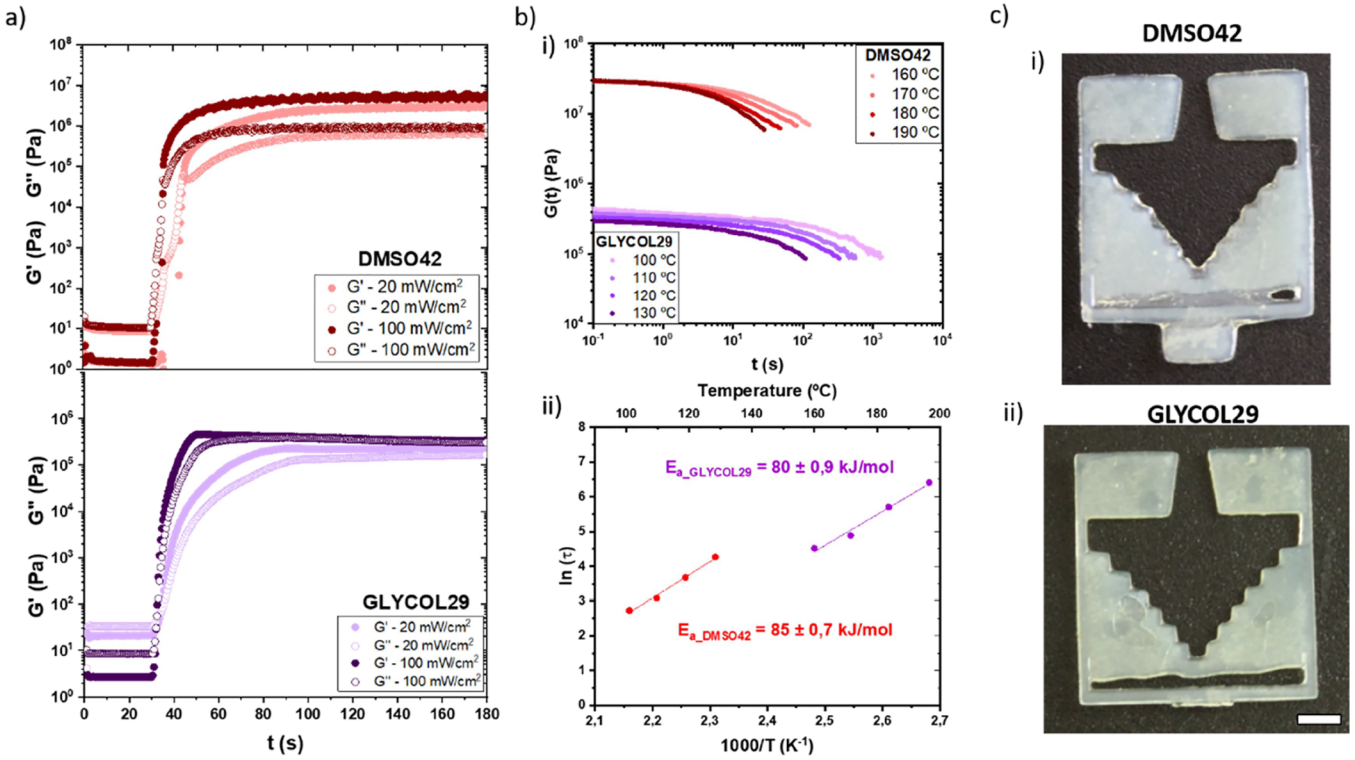

Figure 2. Characterization of the methacrylated vinylogous urethane cross-linker mixed with dimethyl sulfoxide (DMSO) and di(propylene glycol) dimethyl ether (GLYCOL). (a) Irradiated time sweep experiment of the system with DMSO and GLYCOL at different light intensities. (b) Dynamic characterization of the cured material (i) Stress relaxation at different temperatures for both systems and (ii) Arrhenius relationship at different temperatures and (c) printed objects with the methacrylated vinylogous urethane cross-linker mixed with 42 wt % of DMSO and 29 wt % of GLYCOL. The scale bar corresponds to 5 mm.

However, both systems showed a similar activation energy, 80 and 85 kJ/mol (Figure 2b.ii), which suggests that the relaxation is governed by the same amine exchange reaction. On the basis of the success of the photopolymerization process, the resins were also used to explore the possibility for VP. As shown in Figure 2c, reasonable resolution was achieved, thus demonstrating the printability of the resins.

After this proof of concept study and in order to be closer to commercial resins, the possibilities of the vinylogous urethane cross-linker were studied by replacing DMSO and GLYCOL with a reactive methacrylic monomer n-butyl methacrylate (n-BMA). The n-BMA performs a dual function as it reduces the viscosity of the resin before printing but is also copolymerized during photopolymerization, such that it is incorporated into the final structure. Although in this study, n-BMA was used as methacrylic monomer, the nature of the methacrylate monomer can be changed in order to tune the T_g of the resulting network, as demonstrated in our previous work.[42] Similar to the nonreactive diluents, the amount of n-BMA in the system led to significant differences in the initial viscosity, which affects printability. As can be seen in Figure S4, BMA27 showed a higher viscosity compared to the rest of formulations as well as a marked pseudoplastic behavior, which hindered the printability of the system. With a higher concentration of n-BMA, the viscosity was reduced to values more suitable for VP.

The curing kinetics of the n-BMA-based resins were explored by photo-DSC and photorheology. As can be seen in Figure 3a, the photo-DSC experiments showed substantial differences among the four resins. At low quantities of n-BMA (BMA27), the initial resin was highly viscous, and the polymerization contains a large fraction of cross-linking monomer. As a result, the reaction becomes diffusion controlled at relatively low conversion and a limiting conversion of around 50% is reached. As the concentration of n-BMA in the sample increased, the conversion profile showed the characteristic profile of an autoaccelerated process,[45,46] with an initial rate of polymerization followed by a peak at longer times. This behavior can be related to a gel effect, which occurs as the T_g of the monomer/polymer mixture increases above the reaction temperature, leading to a decrease in the rate of termination. As the concentration of n-BMA increases, the acceleration point increases to longer times due to the relatively low T_g of n-BMA (T_g of n-BMA homopolymer is approximately 21 °C). In the case of BMA60, the autoacceleration effect is significantly less pronounced, leading to lower conversions [Figure 3a(ii) and Table 3]. As both BMA60 and BMA27 led to relatively low conversions, they were not further considered in the rest of the work. The results of the photo-DSC experiments are in good agreement with the photorheology experiments using BMA45 and BMA50 resins, where it can be seen that higher concentrations of n-BMA lead to higher gel times (Figure 3b). As expected, when the intensity of the UV light was increased, the gel point slightly shifted to lower times, as can be seen for other energy values in Figures S5 and S6.

3D Printing of Vinylogous Urethane Photoresins. Based on the previous characterization, BMA45 and BMA50 were selected as the most suitable photoresins. Before printing in VP, the optimization of the layer thickness and exposure time was performed by applying the Jacob's equation (eq 1)[40]

https://doi.org/10.1021/acsapm.3c02777
ACS Appl. Polym. Mater. 2024, 6, 2594−2603

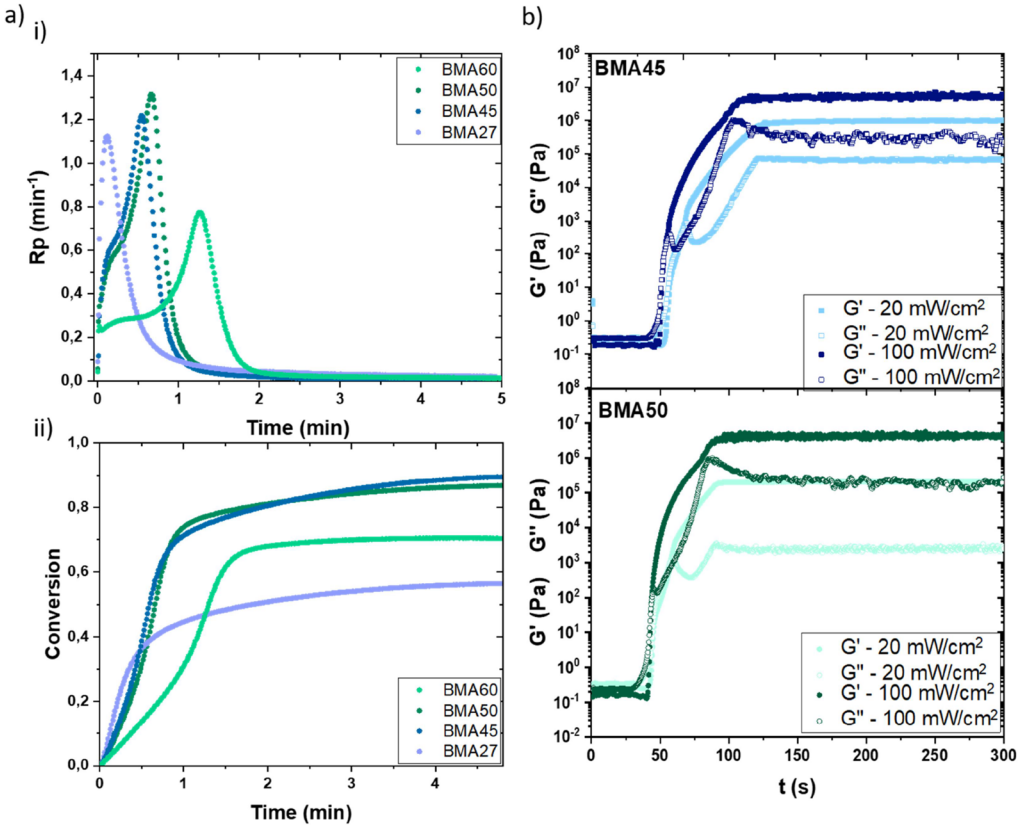

Figure 3. Characterization of the resin with 45 and 50 wt % of n-BMA (a) Photo-DSC (i) Polymerization rate versus time and (ii) Conversion plotted versus time and (b) photorheology.

Table 3. Characterization of the Methacrylated Vinylogous Urethane Cross-Linker with Different Compositions of n-BMA

sample	gel point[a] (s) (100 mW/cm^2)	$R_{p\ max}$ (min^{-1})	conversion	gel content[b] (%)
BMA27	0.47	1.12	0.57	90
BMA45	8.33	1.22	0.90	78
BMA50	13.67	1.32	0.87	76
BMA60	31.26	0.35	0.68	60

[a]Measured at an irradiance of 100 mW/cm^2. [b]For printed films with 1 mm of thickness.

$$C_d = D_p \ln\left(\frac{E}{E_c}\right) \quad (1)$$

where cure depth (C_d) is related to the depth of light penetration into the resin (D_p), which is defined as the depth at which the incident irradiance (I_0) on the resin decreases 37% of its initial value, E is the energy dosage of light for a given layer, and E_c is the critical energy dose of light to form an infinitesimally small gel.[31,47] The exposure time can be directly calculated from the dosage, as it is directly proportional to the exposure time ($E = I_0 \cdot t$), assuming a constant value for the incident irradiance.

In Figure 4a, the Jacob's curves for BMA50 and BMA45 resins are shown. For a preselected layer height of 0.05 mm, an optimum exposure time per layer of 25 s was found for BMA45 (blue trace), while a value of 30 s was found for BMA50 (green trace). The result is in good agreement with PhotoDSC results as the reaction is slower for resins with less vinylogous urethane cross-linker. Taking advantage of this information, the 3D printed shapes shown in Figure 4b were obtained.

Although the application of Jacob's equation is a good starting point for determining the printing conditions of photoresins, further optimization was carried out regarding the obtained XYZ resolution. As reported, methacrylic monomers suffer from shrinkage during the photopolymerization reaction.[48] In order to obtain that information, a 3D object with defined lines of 1000, 500, 250, and 100 μm was printed, and the resulting element was analyzed by SEM as it can be seen in Figure S7. The obtained shrinkage in the XY plane was calculated around 3% ± 1 for BMA50 and 3% ± 2 for BMA45, in good agreement with the one for n-BMA resins.[48] However, significant overcuring problems were detected during printing as shown in (Figure 4c). This shows that, although Jacob's equation can provide valuable information about the printing conditions, it is necessary to perform an optimization in terms of the overcuring of the sample. Following the optimization protocol defined by Page and co-workers,[31] the Z resolution was optimized by incorporating a small concentration of Sudan I (0.05 wt %), a photo absorbent, to the resin. The incorporation of Sudan I resulted in higher exposure times per layer for the printing (Figure 4a) but a significant improvement on the material overcuring (Figure 4d). After the incorporation of Sudan I, we obtained 3D lattices as the ones shown in Figure 4e.ii that with the neat resins were unprintable due to the overcuring problems (Figure 4e.i). Finally, the mechanical characterization of the printed samples was carried out, as shown in Figure S8. Both samples showed brittle behavior with moduli around 1500 MPa, in good agreement with a highly cross-linked material below T_g.

https://doi.org/10.1021/acsapm.3c02777
ACS Appl. Polym. Mater. 2024, 6, 2594−2603

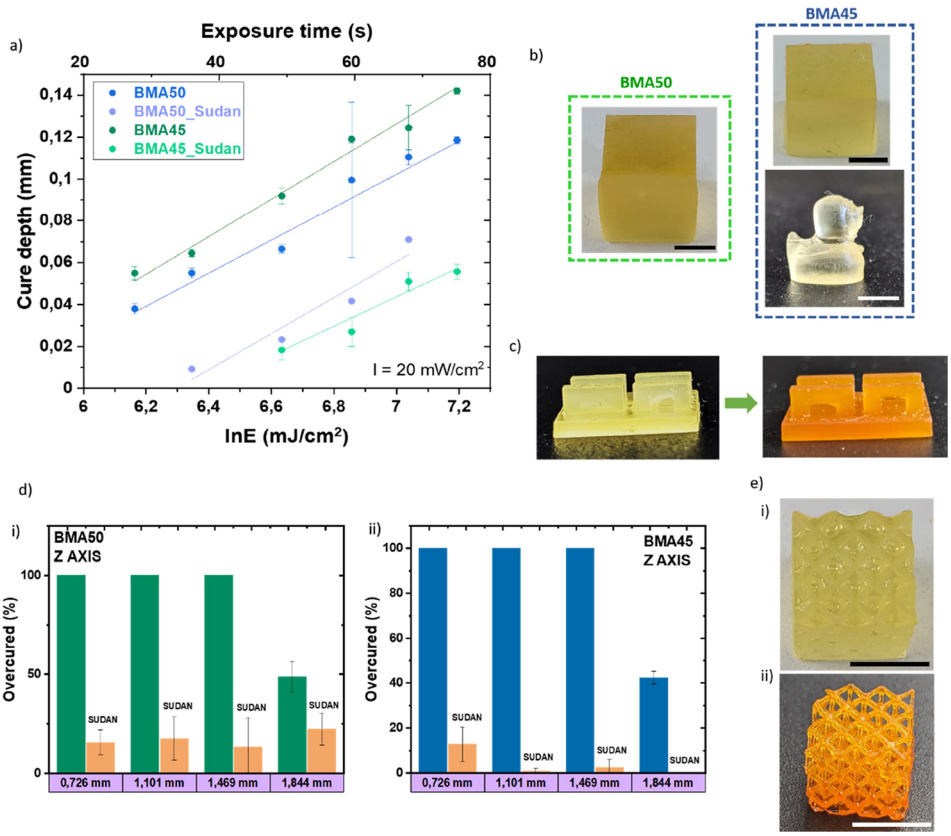

Figure 4. Characterization and optimization of the printed (a) Jacob's curves and its corresponding adjustment for BMA45 and BMA50 with Sudan and without Sudan, (b) 3D pieces obtained following the Jacob's curves for BMA45 and BMA50, and (c) 3D BMA50 pieces printed without Sudan and with Sudan in order to check the overcured in the *Z*-axis, (d.i) Comparation overcured *Z*-axis graph of BMA50 with Sudan and without Sudan, (d.ii) Comparation overcured *Z*-axis graph of BMA45 with Sudan and without Sudan, and (e) Examples of printed pieces of BMA50, (e.i) Without Sudan and (e.ii) with Sudan. The scale bar corresponds to 5 mm.

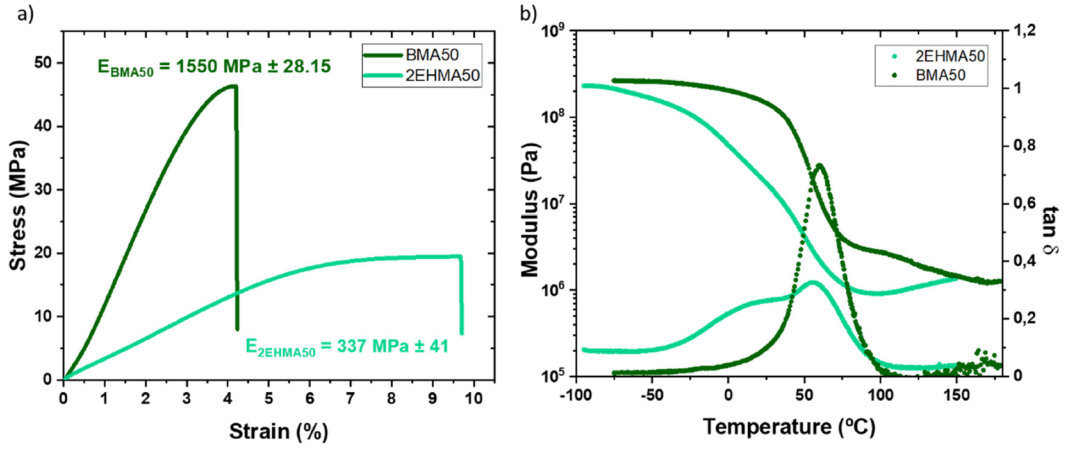

Figure 5. Representative stress strain curves of BMA50 and 2EHMA50. (a, b) Dynamic mechanical thermal analysis of both samples.

As mentioned, the methacrylic nature of the dynamic cross-linker permits tuning the mechanical behavior of the material by simply changing the nature of reactive diluent. Thus, a new resin was synthesized following the same protocol but replacing n-BMA with 2-ethylhexyl methacrylate. As can be seen in Figure 5a, the material shows a lower elastic modulus (340 vs 1500 MPa of n-BMA) and a slightly higher deformation at break (9.5 vs 4% of n-BMA). It is important to point out that the cross-linker amount in our formulation is very high (50 wt %), and consequently, it limits the ductility of the material. This assumption is supported by the DMTA measurements (Figure 5b), where a broad transition was observed for the 2-EHMA sample. The lower transition corresponds to 2-EHMA moieties, while the transition at high temperatures corresponds to the cross-linker. This cross-linker transition was not identified in the n-BMA samples, as they overlapped with the n-BMA transition.

End-of-Use Scenario: Dynamic-Induced Reshaping and Reprinting. The primary interest of CAN materials is their ability to act as a thermoset or thermoplastic under

https://doi.org/10.1021/acsapm.3c02777
ACS Appl. Polym. Mater. 2024, 6, 2594−2603

specific conditions. Therefore, prior to any further analysis of the resin, the dynamic character of the network was explored. One of the simplest ways to determine the dynamic nature of vinylogous urethane networks is through a chemical solubilization of the network. Vinylogous urethane groups are susceptible to a chemical attack through amine groups.[49] In our case, the solubilization of the network structure can occur by reacting an excess of a primary amine, as shown in Figure 6b. Thus, in order to first demonstrate the cross-linked nature

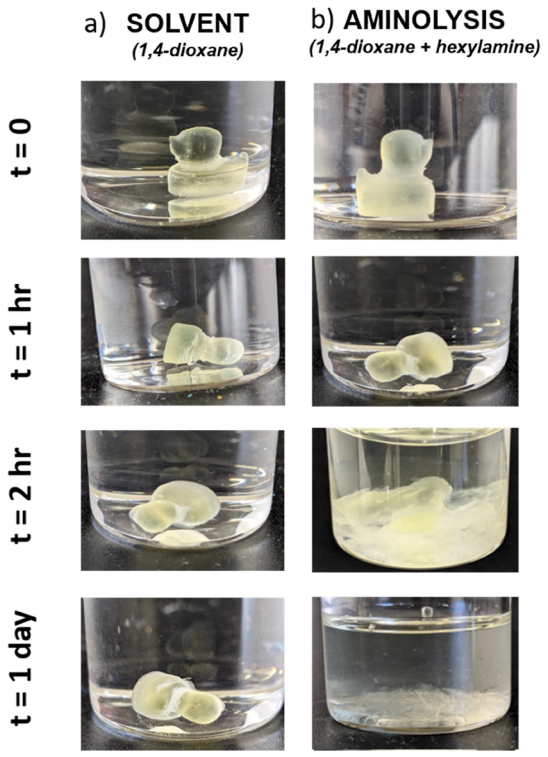

Figure 6. Study of aminolysis reactions: (a) evolution over time of BMA45 in the presence of a nonreactive solvent (1,4-dioxane) and (b) aminolysis process and its evolution over time in a reactive solvent (1,4-dioxane and hexylamine mixture).

of the CAN, a 3D-printed chess tower was introduced in a good solvent for methacrylates (1,4-dioxane) for 24 h at 60 °C. As shown in Figure 6a, the shape remained unaltered. However, when performing the same experiment in the presence of a high excess of 1-hexylamine (1:10 mol ratio referred to vinylogous urethane group in the network), the sample was completely solubilized in 24 h (Figure 6b).

Based on the aminolysis reaction, we studied the possibilities of second generation resins that can be reprinted from our initial formulations. The recycling of the photoresin was conducted in a two-step process (Figure S9a). First, aminolysis was carried out using a bifunctional amine (ethylenediamine) in order to decross link the material and obtain free amine groups in the resulting oligomer mixture. In the second step, AAEMA was added in a 2:1 mol ratio with respect to the added ethylendiamine in order to produce a photoresin with both free methacrylic groups and vinylogous urethane groups, which ensures again the printability of the oligomers and the dynamic character of the resin. The viscosity of the resulting oligomer mixture was adjusted by incorporating n-BMA to improve the printability. By doing so, the resulting mixture was then printed in the form of a film and in a 3D structure (Figure S9b), although the obtained resolution was not optimal. It must be admitted that the proposed process is being an effective recycling alternative since the concentration of cross-linked material in the final process is very low and, furthermore, the material obtained is not chemically similar to the initial one. However, this type of recycling opens the possibility of a second life for acrylic materials polymerized by conventional methods.

The dynamic vitrimer-like character of the samples was confirmed by rheological analysis using both frequency sweeps and stress relaxation tests. As can be seen in Figure 7a.i,ii, for samples BMA45 and BMA50, the stress relaxation occurred on a time scale varying from $\approx 10^2$ to 10^4 s. As expected, the higher the temperature, the lower the relaxation times for the two compositions. This relaxation behavior can also be observed by the minimum in G'' in the frequency sweep (see Figures S10 and S11) followed by an increase at low frequencies. However, the predominantly solid behavior over the frequency range studied reflects the cross-linked nature of the material. On the other hand, it can be observed that as the composition with 45 wt % of n-BMA has higher proportion of the vinylogous urethane cross-linker, the modulus of BMA45 is slightly higher than BMA50. The cross-linked nature of the samples was further confirmed by DMTA, where samples present a constant modulus up to relatively high temperatures (Figures 5 and S12).

In Figure 7b, the activation energy (E_a) at different temperatures for BMA50 and BMA45 obtained through the Arrhenius equation are shown. In this case, the E_a values are around 130 kJ mol^{-1} and 151 kJ mol^{-1} for the polymers that contain 45 and 50 wt % of n-BMA, respectively. The values are in reasonable agreement with previous work using similar vinylogous urethane systems, that ranged between 60 to 162 kJ mol^{-1} depending on the specific chemistry of the network.[49−53] In order to expand the possibilities of these materials, the reprocessing of the printed polymers was carried out by compression molding as shown in Figures 7c and S13 and S14. This demonstrates the potential for postprinting reprocessing and opens up some end-of-life options which are not viable for conventional thermosets produced by VP of acrylic resins. Importantly, the dynamic character of the reprocessed polymer remained unaltered as shown in the relaxation test (Figure 7c).

CONCLUSIONS

In this work, we present vinylogous 3D printable photoresins based on vinylogous urethane cross-linkers. After an initial proof of concept of its viability for VP 3D printing, formulations were developed by mixing the vinylogous urethane cross-linker with n-BMA. In order to ensure correct printability, formulations were optimized in photoresin viscosity and XYZ resolution. Significant overcuring problems were found in printed objects that were overcome by incorporating a low amount of Sudan I as photo absorber. The resulting printed material presented a dynamic behavior, similar to previously reported vinylogous urethane-based materials. It was shown that the materials could be dissolved in the presence of amines as a result of the aminolysis reaction. This reaction was then also explored to allow for the reprinting of the material. To do so, the printed piece was liquefied and functionalized with a methacrylate group, resulting in a second-generation resin that was photopolymerizable. It was also shown that printed specimens could be reshaped at high

https://doi.org/10.1021/acsapm.3c02777
ACS Appl. Polym. Mater. 2024, 6, 2594−2603

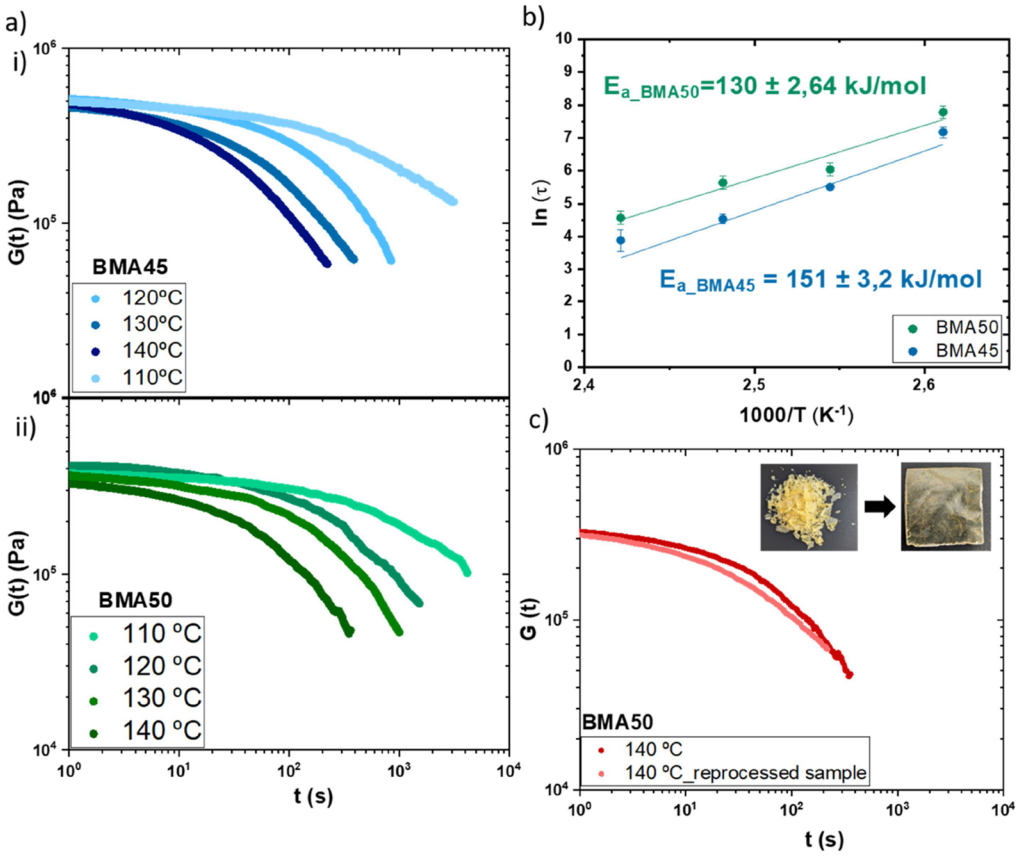

Figure 7. Stress relaxation and Arrhenius relationship (a) representative stress relaxation curves at various temperatures of BMA50 and BMA45, (b) Arrhenius relationship and the activation energy of the composition with a 50 and 45 wt % of n-BMA, (c) Comparison between an original and reprocessed sample of BMA50 with its stress relaxation curve at 140 °C.

temperature upon application of pressure while retaining the dynamic character of freshly printed materials.

The authors recognize funding provided by the Spanish government (Grant PID2019−107889GA-100 funded by MCIN/AEI/10.13039/501100011033) and the Basque Government (IT1503-22, KK-2023/00054, and PIBA_2021_39). The authors want to thank I. Ruiz de Eguino (Mondragon University) for the spectral characterization of the light sources and I. Insua for helping with the design of the 3D objects.

■ ASSOCIATED CONTENT

Supporting Information

The Supporting Information is available free of charge at https://pubs.acs.org/doi/10.1021/acsapm.3c02777.

Additional information regarding rheological and mechanical characterization as well as reprinting process. Light source output spectra for photorheology accessory and Asiga 3D printer; ^{13}C NMR spectra of the starting materials and synthesized methacrylic vinylogous urethane cross-linker; viscosity curves for different compositions; viscosity curves for different compositions of butyl methacrylate; photorheology of BMA45 at different energy exposure; photorheology of BMA50 at different energy exposure; and characterization and optimization of the printed pieces (PDF)

■ AUTHOR INFORMATION

Corresponding Authors

Nicholas Ballard − *POLYMAT and University of the Basque Country (UPV/EHU), 20018 Donostia-San Sebastián, Spain; Ikerbasque, Basque Foundation for Science, 48009 Bilbao, Spain;* orcid.org/0000-0002-9480-2922; Email: nicholas.ballard@polymat.eu

Robert Aguirresarobe − *POLYMAT and Department of Advanced Polymers and Materials: Physics, Chemistry and Technology, Faculty of Chemistry, University of the Basque Country (UPV/EHU), 20018 Donostia-San Sebastián, Spain;* orcid.org/0000-0001-9736-9098; Email: roberto.hernandez@ehu.eus

Authors

Laura Ballester-Bayarri − *POLYMAT and Department of Advanced Polymers and Materials: Physics, Chemistry and Technology, Faculty of Chemistry, University of the Basque Country (UPV/EHU), 20018 Donostia-San Sebastián, Spain*

Alodi Pascal − *POLYMAT and Department of Advanced Polymers and Materials: Physics, Chemistry and Technology, Faculty of Chemistry, University of the Basque Country (UPV/EHU), 20018 Donostia-San Sebastián, Spain;* orcid.org/0009-0002-6781-2890

Jon Ayestaran − *POLYMAT and Department of Advanced Polymers and Materials: Physics, Chemistry and Technology, Faculty of Chemistry, University of the Basque Country (UPV/EHU), 20018 Donostia-San Sebastián, Spain*

https://doi.org/10.1021/acsapm.3c02777
ACS Appl. Polym. Mater. 2024, 6, 2594−2603

Alba Gonzalez − *POLYMAT and Department of Advanced Polymers and Materials: Physics, Chemistry and Technology, Faculty of Chemistry, University of the Basque Country (UPV/EHU), 20018 Donostia-San Sebastián, Spain;* orcid.org/0000-0003-2513-8754

Complete contact information is available at: https://pubs.acs.org/10.1021/acsapm.3c02777

Notes

The authors declare no competing financial interest.

REFERENCES

(1) Bowman, C. N.; Kloxin, C. J. Covalent adaptable networks: reversible bond structures incorporated in polymer networks. *Angew. Chem., Int. Ed.* **2012**, *18* (51), 4272−4274.
(2) Kloxin, C. J.; Scott, T. F.; Adzima, B. J.; Bowman, C. N. Covalent adaptable networks (CANs): a unique paradigm in cross-linked polymers. *Macromolecules* **2010**, *43* (6), 2643−2653.
(3) Kloxin, C. J.; Bowman, C. N. Covalent adaptable networks: smart, reconfigurable and responsive network systems. *Chem. Soc. Rev.* **2013**, *42* (17), 7161−7173.
(4) Zhang, Z. P.; Rong, M. Z.; Zhang, M. Q. Polymer engineering based on reversible covalent chemistry: A promising innovative pathway towards new materials and new functionalities. *Prog. Polym. Sci.* **2018**, *80*, 39−93.
(5) Zhang, V.; Kang, B.; Accardo, J. V.; Kalow, J. A. Structure−reactivity−property relationships in covalent adaptable networks. *J. Am. Chem. Soc.* **2022**, *144* (49), 22358−22377.
(6) Podgórski, M.; Fairbanks, B. D.; Kirkpatrick, B. E.; McBride, M.; Martinez, A.; Dobson, A.; Bongiardina, N. J.; Bowman, C. N. Toward Stimuli-Responsive Dynamic Thermosets through Continuous Development and Improvements in Covalent Adaptable Networks (CANs). *Adv. Mater.* **2020**, *32* (20), No. e1906876.
(7) Aguirresarobe, R. H.; Nevejans, S.; Reck, B.; Irusta, L.; Sardon, H.; Asua, J. M.; Ballard, N. Healable and self-healing polyurethanes using dynamic chemistry. *Prog. Polym. Sci.* **2021**, *114*, No. 101362.
(8) Chakma, P.; Konkolewicz, D. Dynamic covalent bonds in polymeric materials. *Angew. Chem., Int. Ed.* **2019**, *58* (29), 9682−9695.
(9) Winne, J. M.; Leibler, L.; Du Prez, F. E. Dynamic covalent chemistry in polymer networks: a mechanistic perspective. *Polym. Chem.* **2019**, *10* (45), 6091−6108.
(10) Scheutz, G. M.; Lessard, J. J.; Sims, M. B.; Sumerlin, B. S. Adaptable crosslinks in polymeric materials: resolving the intersection of thermoplastics and thermosets. *J. Am. Chem. Soc.* **2019**, *141* (41), 16181−16196.
(11) Sridhar, L. M.; Oster, M. O.; Herr, D. E.; Gregg, J. B.; Wilson, J. A.; Slark, A. T. Re-usable thermally reversible crosslinked adhesives from robust polyester and poly (ester urethane) Diels−Alder networks. *Green Chem.* **2020**, *22* (24), 8669−8679.
(12) Erice, A.; de Luzuriaga, A. R.; Azcune, I.; Fernandez, M.; Calafel, I.; Grande, H.-J.; Rekondo, A. New injectable and self-healable thermoset polythiourethane based on S-aromatic thiourethane dissociative exchange mechanism. *Polymer* **2020**, *196*, No. 122461.
(13) Taplan, C.; Guerre, M.; Winne, J. M.; Du Prez, F. E. Fast processing of highly crosslinked, low-viscosity vitrimers. *Materials Horizons* **2020**, *7* (1), 104−110.
(14) Qiu, J.; Ma, S.; Wang, S.; Tang, Z.; Li, Q.; Tian, A.; Xu, X.; Wang, B.; Lu, N.; Zhu, J. Upcycling of polyethylene terephthalate to continuously reprocessable vitrimers through reactive extrusion. *Macromolecules* **2021**, *54* (2), 703−712.
(15) Li, C.; Ju, B.; Zhang, S. Twin-screw extrusion molding of a cellulose-based vitrimer containing a crosslinkable macromolecular plasticizer. *Int. J. Biol. Macromol.* **2023**, *225*, 1487−1493.
(16) Joosten, L. M. A.; Cassagnau, P.; Drockenmuller, E.; Montarnal, D. Synthesis, Recycling and High-Throughput Reprocessing of Phase-Separated Vitrimer-Thermoplastic Blends. *Adv. Funct. Mater.* **2023**, *34*, No. 2306882.
(17) Zhu, G.; Houck, H. A.; Spiegel, C. A.; Selhuber-Unkel, C.; Hou, Y.; Blasco, E. Introducing Dynamic Bonds in Light-based 3D Printing. *Adv. Funct. Mater.* **2023**, No. 2300456.
(18) Rossegger, E.; Höller, R.; Reisinger, D.; Strasser, J.; Fleisch, M.; Griesser, T.; Schlögl, S. Digital light processing 3D printing with thiol−acrylate vitrimers. *Polym. Chem.* **2021**, *12* (5), 639−644.
(19) Joe, J.; Shin, J.; Choi, Y. S.; Hwang, J. H.; Kim, S. H.; Han, J.; Park, B.; Lee, W.; Park, S.; Kim, Y. S. A 4D Printable Shape Memory Vitrimer with Repairability and Recyclability through Network Architecture Tailoring from Commercial Poly(ε-caprolactone). *Adv. Sci.* **2021**, *8* (24), No. 2103682.
(20) Choi, S.; Park, B.; Jo, S.; Seo, J. H.; Lee, W.; Kim, D.-G.; Lee, K. B.; Kim, Y. S.; Park, S. Weldable and Reprocessable Shape Memory Epoxy Vitrimer Enabled by Controlled Formulation for Extrusion-Based 4D Printing Applications. *Adv. Eng. Mater.* **2022**, *24* (4), 2101497.
(21) Niu, W.; Zhang, Z.; Chen, Q.; Cao, P.-F.; Advincula, R. C. Highly recyclable, mechanically isotropic and healable 3D-printed elastomers via polyurea vitrimers. *ACS Materials Letters* **2021**, *3* (8), 1095−1103.
(22) Shaukat, U.; Sölle, B.; Rossegger, E.; Rana, S.; Schlögl, S. Vat photopolymerization 3D-printing of dynamic thiol-acrylate photopolymers using bio-derived building blocks. *Polymers* **2022**, *14* (24), 5377.
(23) Bijalwan, V.; Rana, S.; Yun, G. J.; Singh, K. P.; Jamil, M.; Schlögl, S. 3D Printing of Covalent Adaptable Networks: Overview, Applications and Future Prospects. *Polym. Rev.* **2023**, 1−44.
(24) Kim, S.; Rahman, M. A.; Arifuzzaman, M.; Gilmer, D. B.; Li, B.; Wilt, J. K.; Lara-Curzio, E.; Saito, T. Closed-loop additive manufacturing of upcycled commodity plastic through dynamic cross-linking. *Sci. Adv.* **2022**, *8* (22), No. eabn6006.
(25) Saed, M. O.; Lin, X.; Terentjev, E. M. Dynamic semicrystalline networks of polypropylene with thiol-anhydride exchangeable cross-links. *ACS Appl. Mater. Interfaces* **2021**, *13* (35), 42044−42051.
(26) Prasanna Kar, G.; Lin, X.; Terentjev, E. M. Fused Filament Fabrication of a Dynamically Crosslinked Network Derived from Commodity Thermoplastics. *ACS Applied Polymer Materials* **2022**, *4* (6), 4364−4372.
(27) Pagac, M.; Hajnys, J.; Ma, Q.; Jancar, L.; Jansa, J.; Stefek, P.; Mesicek, J. A review of vat photopolymerization technology: Materials, applications, challenges, and future trends of 3D printing. *Polymers* **2021**, *13*, 598.
(28) Melchels, F. P.; Feijen, J.; Grijpma, D. W. A review on stereolithography and its applications in biomedical engineering. *Biomaterials* **2010**, *31* (24), 6121−6130.
(29) Krishna Kumar, B.; Dickens, T. J. Dynamic bond exchangeable thermoset vitrimers in 3D-printing. *J. Appl. Polym. Sci.* **2023**, *140* (2), No. e53304.
(30) Vazquez-Martel, C.; Becker, L.; Liebig, W. V.; Elsner, P.; Blasco, E. Vegetable Oils as Sustainable Inks for Additive Manufacturing: A Comparative Study. *ACS Sustainable Chem. Eng.* **2021**, *9* (49), 16840−16848.
(31) Stevens, L. M.; Recker, E. A.; Zhou, K. A.; Garcia, V. G.; Mason, K. S.; Tagnon, C.; Abdelaziz, N.; Page, Z. A. Counting All Photons: Efficient Optimization of Visible Light 3D Printing. *Adv. Mater. Technol.* **2023**, *8*, No. 2300052.
(32) Schwartz, J. J. Additive manufacturing: Frameworks for chemical understanding and advancement in vat photopolymerization. *MRS Bull.* **2022**, *47* (6), 628−641.
(33) Yee, D. W.; Greer, J. R. Three-dimensional chemical reactors: in situ materials synthesis to advance vat photopolymerization. *Polym. Int.* **2021**, *70* (7), 964−976.
(34) Robinson, L. L.; Self, J. L.; Fusi, A. D.; Bates, M. W.; Read de Alaniz, J.; Hawker, C. J.; Bates, C. M.; Sample, C. S. Chemical and mechanical tunability of 3D-printed dynamic covalent networks based on boronate esters. *ACS Macro Lett.* **2021**, *10* (7), 857−863.

(35) Zhang, B.; Kowsari, K.; Serjouei, A.; Dunn, M. L.; Ge, Q. Reprocessable thermosets for sustainable three-dimensional printing. *Nat. Commun.* **2018**, *9* (1), 1831.
(36) Cui, C.; An, L.; Zhang, Z.; Ji, M.; Chen, K.; Yang, Y.; Su, Q.; Wang, F.; Cheng, Y.; Zhang, Y. Reconfigurable 4D printing of reprocessable and mechanically strong polythiourethane covalent adaptable networks. *Adv. Funct. Mater.* **2022**, *32* (29), No. 2203720.
(37) Zhao, B.; Hao, C.; Chang, Y. C.; Cao, Y.; Liu, T.; Fei, M.; Shao, L.; Zhang, J. Photo-Curing 3D Printing of Thermosetting Sacrificial Tooling for Fabricating Fiber-Reinforced Hollow Composites. *Adv. Funct. Mater.* **2023**, *33*, No. 2213663.
(38) Miao, J.-T.; Ge, M.; Wu, Y.; Peng, S.; Zheng, L.; Chou, T. Y.; Wu, L. 3D printing of sacrificial thermosetting mold for building near-infrared irradiation induced self-healable 3D smart structures. *Chemical Engineering Journal* **2022**, *427*, No. 131580.
(39) Zhu, G.; Zhang, J.; Huang, J.; Qiu, Y.; Liu, M.; Yu, J.; Liu, C.; Shang, Q.; Hu, Y.; Hu, L. Recyclable and reprintable biobased photopolymers for digital light processing 3D printing. *Chem. Eng. J.* **2023**, *452*, No. 139401.
(40) Peng, S.; Wang, Z.; Lin, J.; Miao, J. T.; Zheng, L.; Yang, Z.; Weng, Z.; Wu, L. Tailored and highly stretchable sensor prepared by crosslinking an enhanced 3D printed UV-curable sacrificial mold. *Adv. Funct. Mater.* **2021**, *31* (10), No. 2008729.
(41) Fang, Z.; Shi, Y.; Mu, H.; Lu, R.; Wu, J.; Xie, T. 3D printing of dynamic covalent polymer network with on-demand geometric and mechanical reprogrammability. *Nat. Commun.* **2023**, *14* (1), 1313.
(42) Ballester-Bayarri, L.; Limousin, E.; Fernández, M.; Aguirresarobe, R.; Ballard, N. Scalable synthesis of methacrylate-based vitrimer powders by suspension polymerization. *Polym. Chem.* **2023**, *14* (14), 1656−1664.
(43) Lessard, J. J.; Garcia, L. F.; Easterling, C. P.; Sims, M. B.; Bentz, K. C.; Arencibia, S.; Savin, D. A.; Sumerlin, B. S. Catalyst-free vitrimers from vinyl polymers. *Macromolecules* **2019**, *52* (5), 2105−2111.
(44) Harikrishna, R. Inhibition effect of N, N-diglycidyl-4-glycidyloxy aniline on photosensitized cationic polymerization of formulations involving resorcinol diglycidyl ether and poly (propylene glycol) diglycidyl ether. *J. Photochem. Photobiol., A* **2015**, *303*, 17−27.
(45) Achilias, D. S. A review of modeling of diffusion controlled polymerization reactions. *Macromol. Theory Simul.* **2007**, *16* (4), 319−347.
(46) Achilias, D.; Kiparissides, C. Development of a general mathematical framework for modeling diffusion-controlled free-radical polymerization reactions. *Macromolecules* **1992**, *25* (14), 3739−3750.
(47) Jacobs, P. F. Fundamentals of stereolithography. In *1992 international solid freeform fabrication symposium*, 1992.
(48) Rusu, M.; Rusu, D.; Rusu, M.; Ichim, I. Properties of acrylic bone cements modified with poly (butyl methacrylate). *J. Optoelectron. Adv. Mater.* **2010**, *12* (2), 339.
(49) Denissen, W.; Rivero, G.; Nicolaÿ, R.; Leibler, L.; Winne, J. M.; Du Prez, F. E. Vinylogous urethane vitrimers. *Adv. Funct. Mater.* **2015**, *25* (16), 2451−2457.
(50) Denissen, W.; Droesbeke, M.; Nicolaÿ, R.; Leibler, L.; Winne, J. M.; Du Prez, F. E. Chemical control of the viscoelastic properties of vinylogous urethane vitrimers. *Nat. Commun.* **2017**, *8* (1), 14857.
(51) Engelen, S.; Wróblewska, A. A.; De Bruycker, K.; Aksakal, R.; Ladmiral, V.; Caillol, S.; Du Prez, F. E. Sustainable design of vanillin-based vitrimers using vinylogous urethane chemistry. *Polym. Chem.* **2022**, *13* (18), 2665−2673.
(52) Ma, Y.; Jiang, X.; Shi, Z.; Berrocal, J. A.; Weder, C. Closed-Loop Recycling of Vinylogous Urethane Vitrimers. *Angew. Chem., Int. Ed.* **2023**, *62* (36), No. e202306188.
(53) Spiesschaert, Y.; Danneels, J.; Van Herck, N.; Guerre, M.; Acke, G.; Winne, J.; Du Prez, F. Polyaddition synthesis using alkyne esters for the design of vinylogous urethane vitrimers. *Macromolecules* **2021**, *54* (17), 7931−7942.

https://doi.org/10.1021/acsapm.3c02777
ACS Appl. Polym. Mater. 2024, 6, 2594−2603